GeoConvention 2015
GEOSCIENCE
new horizons
Telus Convention Centre • 4-8 May 2015 • Calgary, AB Canada

2D finite-difference microseismic simulations: Effects of path and source

Hoda Rashedi and David W. Eaton
Department of Geoscience, University of Calgary

Summary

We present a suite of 2.5-D synthetic microseismic events computed using three different velocity models, representative of Horn River, Montney and Central Alberta regions of western Canada. This study aims to establish finite-difference templates for microseismicity in these areas. We use an explicit second-order finite-difference (FD) method that is capable of handling general anisotropy, up to triclinic symmetry. The microseismic source is specified as an arbitrary moment tensor, subject to the constraint that the source is located in an isotropic layer. Although our algorithm allows for more general anisotropy (possible only if sufficient a priori information is available), the anisotropy considered is primarily confined to transverse isotropy with a vertical symmetry axis (VTI).This anisotropic scenario is well suited to modeling wave propagation in shale.

We have calculated synthetic seismographs for both surface and downhole cases. Care is required to avoid contamination of the synthetic data by edge reflections, which are problematic due to the ineffectiveness of currently known FD absorbing boundary for general anisotropy. For geophone arrays deployed at the surface, we use a coarser mesh and apply a post-simulation filter to account for a highly attenuating near-surface layer. A set of random event locations and varying moment tensors are used.

Introduction

Synthetic seismograms for a realistic scenario provide an effective way to benchmark processing and interpretation algorithms. In exploration seismology, an excellent example is provided by the Marmousi dataset, a prestack acoustic finite-difference dataset created by IFP in 1988 [Bourgeois et al.,1991], shown in Figure1. This model has since been used in 100's of publications to benchmark and test migration codes, including sensitivity of prestack depth migration to the velocity model [Versteeg,1993], anisotropic [Alkhalifah, 1997] and elastic effects [Martin et al., 2006]. Thus, the Marmousi model has been extensively used as a calibration tool to test various algorithms.

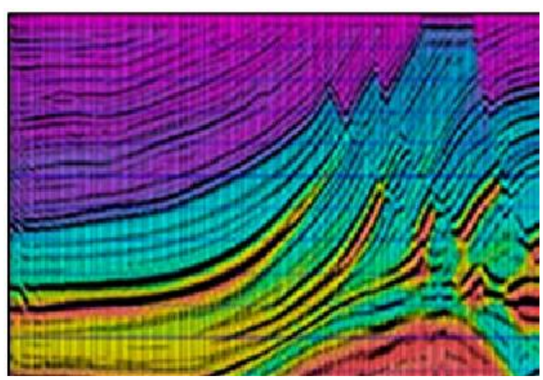

Figure 1: Prestack FD dataset created by IFP in 1988

Numerous lithologies exhibit variable physical properties (velocity, anisotropy, etc) [Thomsen, 1986] that affect wave propagation from the source to the receivers. In order to calculate microseismic event locations effectively, accurate velocity and anisotropy models are essential. Typically this information must be inferred from other sources such as well logs, surface seismic velocity data or from adjustment of velocity models based on relatively sparse calibration shots. Since this problem is generally highly underconstrained, the background model is generally not sufficiently well known to adequately distinguish different sources of errors. The objective of the present study is to create a realistic suite of synthetic microseismograms for a scenario in which the source location, mechanism and background model are known and the complete wavefield containing multiples, guided waves etc. is accurately simulated. To achieve this goal, we have modified a 3D anisotropic (an)elastic finite-difference method [Boyd, 2006] to allow for:

- localized moment-tensor source
- VTI anisotropy [Thomsen1986]

This paper provides a brief description of the method used to generate a suite of synthetic micro-seismograms for a set of different locations and variable moment tensors.

Theory

The equation of motion in an elastic medium can be represent by:

$$(C_{ijkl}U_{k,l})_{,j} - \rho \ddot{U}_j = 0$$

where C_{ijkl} is the stiffness tensor, U is the displacement and ρ is the density of the medium. Also note that the dots in this notation represent the time derivatives and *",j"* subscript denotes the partial derivative of *j*th component. Both anisotropy and velocity are considered in this equation.

There are various numerical methods to solve the wave equation in order to model the seismic wave propagation in realistic media [e.g., Semblat 2011, Bohlen, 2002]. Finite-difference methods have been widely used to solve the wave equation and model the wave propagation [Juhlin, 1995, Kelly et al., 1976]. In principle, this numerical approach simulates wave propagation in different time intervals subject to prescribed boundary constraints.

In this study we have used the finite-difference method (FDM) for modeling the wave propagation because it allows a fully arbitrary model which provides for a full set of surface multiples, focusing and defocusing of seismic waves, wave front healing, and complex frequency-dependent effects to be observed [Boyd, 2006]. As always, with this method care is required to avoid artifacts resulting from numerical instability and imperfect boundary conditions [Boyd, 2006].

Examples

A common type of microseismic source is represented by the double couple moment tensor, which can be expressed in the form

$$M_{DC} = \begin{bmatrix} 0 & 0 & 1 \\ 0 & 0 & 0 \\ 1 & 0 & 0 \end{bmatrix} .$$

The nonzero X and Z component of this moment tensor have been chosen to represent the bedding parallel horizontal shear stress.

A source-type (Hudson) plot of this pure double couple moment tensor is shown in Figure 2 (left panel), which is centered at the origin and indicate pure shear slip. The middle and right panel in Figure 2 shows two stages of wave-field snapshots for down-hole arrays in which P-waves and S-waves can clearly be distinguished. Colors in these diagrams represent the amplitude of wave during propagation. The P-wave radiation pattern is characterized by mutually perpendicular nodal planes, across which the polarity undergoes a reversal.

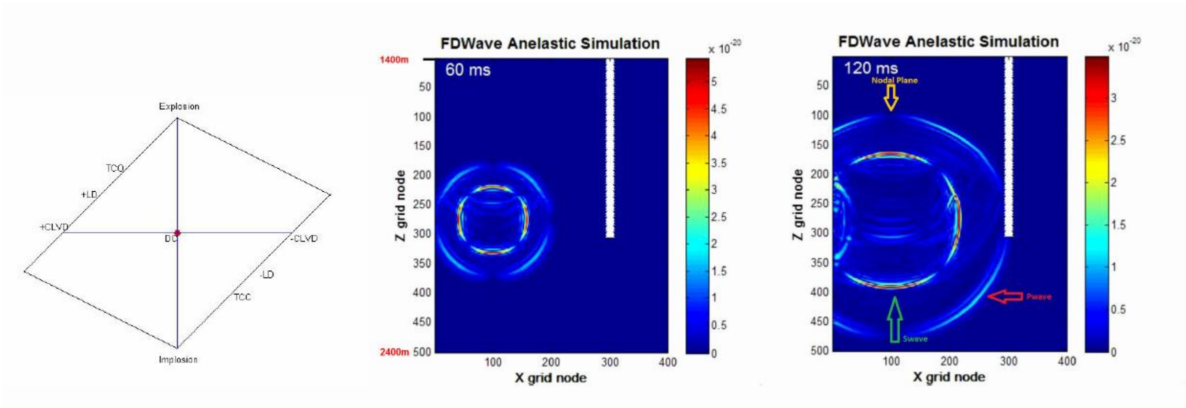

Figure 2: Left panel: The Hudson plot of the double-couple source used for this simulation. Middle panel: Snapshot of the wave propagation in an isotropic medium at 60ms, showing reflection at a velocity boundary. Axis labels show node index while the red numbers indicate the depth of the top and bottom of the model frame. Right panel: Snapshot of the same simulation at 120ms. Note downgoing reflection from a layer boundary the side-reflection boundary artifact.

Figure 3 shows x- and z-component record sections calculated for the vertical receiver array depicted in Figure 2, which represents an isotropic model. The record sections are dominated by P and S direct arrivals. The P wave arrival has the highest amplitudes on the x-component, as expected due to the near-horizontal propagation from source to receiver. Conversely, the S-wave direct arrival is strongest on the z-component, due to the transverse orientation of S-wave. Up-going P-S model conversions are also evident.

Interpreting these record sections in tandem with wave-field snapshots provides a powerful tool to understand the interaction of microseismic wave-fields and source radiation patterns with heterogeneous media.

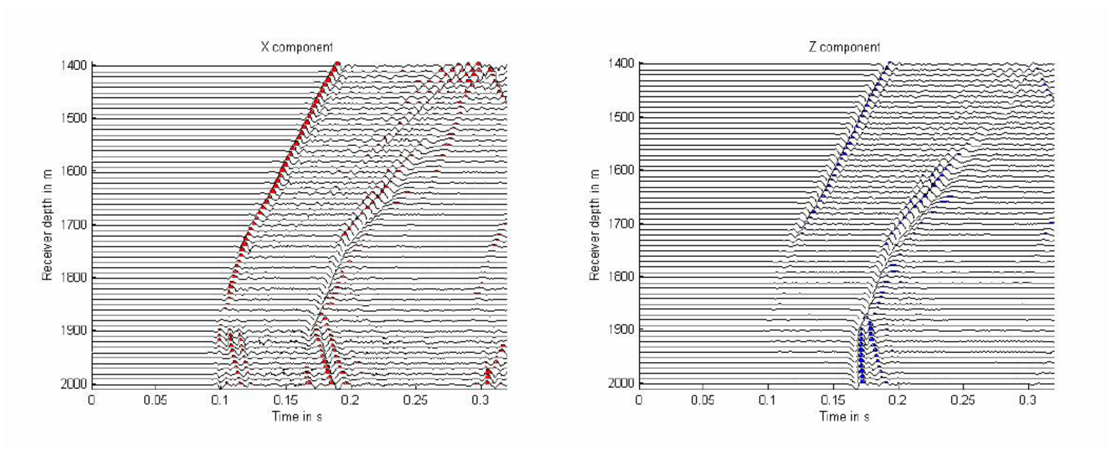

Figure 3: Synthetic record sections for a downhole receiver array. In the X component diagram, the P-waves exhibit stronger amplitudes, as they propagate horizontally. Likewise, S waves are stronger in Z component image.

Conclusions

Case studies of finite-difference simulations involving various source types and positions incorporating varying degrees of anisotropy can provide valuable insights into behaviour of the wave from microseismic event. Here, we computed 2D synthetic microseismic data using a FDM with general anisotropy and interpreted their record sections. This approach enables analysis and identification of wave-field elements such as head waves, post-critical reflections and guided waves. Imperfect absorbing boundaries create artifacts that require model dimensions to be extended to ensure that artifacts do not interfere with desired signals.

Acknowledgements

The original idea for this project was proposed by Francois Aubin. Shawn Maxwell and Emmanual Auger provided further input. Chad Hogan, Mohamed Sameen, Jubran Akram and Kim Pike contributed ideas and some of the codes used. We thank sponsors of the Microseismic Industry Consortium for funding this project.

References

T. Alkhalifah. An anisotropic Marmousi model. Stanford Exploration Project, report 95:265-283, 1997.

T. Bohlen. Parallel 3d viscoelastic finite-difference seismic modeling. Computers and Geosciences, 28: 887-899, 2002.

A. Bourgeois, M. Bourget, P. Lailly, M. Poulet, P. Ricarte, and R. Versteeg. Marmousi, model and data. Proceedings of the 1990 EAGE workshop on Practical Aspects of Seismic Data Inversion: Eur. Assoc. Expl. Geophys, 5-16, 1991.

O. Boyd. An efficient matlab script to calculate heterogeneous anisotropically elastic wave propagation in three dimensions. Comp. Geosci, 32: 259-264, 2006.

C. Juhlin. Finite-difference elastic wave propagation in 2d heterogeneous transversely isotropic media. Geophysical Prospecting, 43: 843-858, 1995.

K. R. Kelly, R. Ward, S. Treitel, and R. Alford. Synthetic seismograms: A finite-difference approach. Geophysics, 41: 2-27, 1976.

G. Martin, R. Wiley, and K. Marfurt. Marmousi2: An elastic upgrade for Marmousi. The Leading Edge, 25(2): 156-166., 2006.

J. F. Semblat. Modeling seismic wave propagation and amplification in 1d/2d/3d linear and nonlinear unbounded media. Int. J. Geomechanics 11: 440-448, 2011.

L. Thomsen. Weak elastic anisotropy. Geophysics, 51: 1954-1966, 1986.

R. J. Versteeg. Sensitivity of prestack depth migration to the velocity model. Geophysics, 58: 873-882, 1993.